Compound I Formation in Artichoke (*Cynara scolymus* L.) Peroxidase Is Modulated by the Equilibrium between Pentacoordinated and 6-Aquo Hexacoordinated Forms of the Heme and by Calcium Ions†

Alexander N. P. Hiner,§ Lara Sidrach,§ Soledad Chazarra,§ Ramón Varón,⊥ José Tudela,§ Francisco García-Cánovas,§ and José Neptuno Rodríguez-López*,§

Grupo de Enzimología (GENZ), Departamento de Bioquímica y Biología Molecular-A, Facultad de Biología, Universidad de Murcia, Murcia, Spain, and Departamento de Química-Física, Escuela Técnica Superior de Albacete, Universidad de Castilla-La Mancha, Albacete, Spain

Received April 11, 2003

ABSTRACT: Basic artichoke (*Cynara scolymus* L.) peroxidase (AKP-C), when purified from the plant, has an unusually intense and sharp Soret absorption peak. The resonance Raman spectrum [López-Molina, D., et al. (2003) *J. Inorg. Biochem. 94*, 243−254] suggested a mixture of pentacoordinate high-spin (5cHS) and 6-aquo hexacoordinate high-spin (6cHS) ferric heme species. The rate constant (k_1) of compound I formation with hydrogen peroxide (H_2O_2) was also lower than expected. Further stopped-flow studies have shown this reaction to be biphasic: a nonsaturating fast phase and a slow phase with complex H_2O_2 concentration dependence. Addition of calcium ions (Ca^{2+}) changed the absorption spectrum, suggesting the formation of a fully 5cHS species with a k_1 more than 5 orders of magnitude greater than that in the absence of Ca^{2+} using the chelator ethylenediaminetetraacetic acid. Ca^{2+} titrations gave a dissociation constant for a single Ca^{2+} of approximately 20 μM. The circular dichroism spectrum of AKP-C was not significantly altered by Ca^{2+}, indicating that any structural changes will be minor, but removal of Ca^{2+} did suppress the alkaline transition between pH 10 and 11. A kinetic analysis of the reaction of Ca^{2+}-free AKP-C with H_2O_2 supports an equilibrium between a slow-reacting 6cHS form and a more rapidly reacting 5cHS species, the presence of which was confirmed in nonaqueous solution. AKP-C, as purified, is a mixture of Ca^{2+}-bound 5cHS, 6-aquo 6cHS, and Ca^{2+}-free 5cHS species. The possibility that Ca^{2+} concentration could control peroxidase activity in the plant is discussed.

Homologous heme peroxidases are found in plants, fungi, and prokaryotes (*1*−*3*) and have been identified playing roles in processes as diverse as the removal of hydrogen peroxide (H_2O_2)[1] and other oxidant species (class I peroxidases of prokaryotic origin including catalase-peroxidase, yeast cytochrome *c* peroxidase, and ascorbate peroxidase) (*4*−*6*), lignin digestion (class II peroxidases from fungi such as *Coprinus cinereus* and *Phanerochaete chrysosporium* (LiP)) (*7*, *8*), and biosynthesis and pathogen defense (class III secretory plant peroxidases such as that from horseradish roots (HRP)) (*9*−*13*).

Despite the wide range of processes catalyzed by different heme peroxidases, the general reaction mechanism is similar and has traditionally been considered to occur in three irreversible steps (*9*). The first of these steps is the two-electron oxidation of ferric peroxidase by H_2O_2 to form compound I, which is followed by two single-electron reduction steps of this intermediate by the second (reducing) substrate, regenerating resting enzyme and forming product. Thus, generally, two moles of reducing substrate are oxidized by one mole of H_2O_2. Compound I (formal oxidation state 5+) contains an oxyferryl iron (Fe(IV)═O) center and a radical delocalized either on the porphyrin ring (π-cation radical) (*14*) or on an amino acid (normally tryptophan) side chain (*15*, *16*). In recent years, work to elucidate the mechanism of compound I formation and probe its structure has continued. These studies have revealed enzyme−H_2O_2 complex formation followed by heterolytic H_2O_2 cleavage to yield compound I and water (*17*−*20*). Other work has examined the localization and stability of the radical (*15*, *16*, *21*−*24*). However, under stopped-flow experimental conditions, compound I formation is normally observed as a single-step process with an apparent second-order rate constant, in the case of a typical class III peroxidase such as HRP-C of $k_1 > 1 \times 10^7$ M^{-1} s^{-1} (*3*, *9*).

Compound I is a highly reactive oxidant species, and enzyme specificity is controlled at a biochemical level mainly

† This research was supported by grants from the Ministerio de Ciencia y Technología (Spain), project AGL2002-01255 to F.G.-C. and J.N.R.-L., and project BQU2002-01960 to R.V., and the Fundación Seneca (Murcia, Spain), project PI-79/00810/FS/01 to J.T. and J.N.R.-L. S.C. and A.N.P.H. are supported by contracts with ArtBiochem S.L. (Murcia, Spain). L.S. has a grant from the Ministerio de Educación y Cultura (Spain).

* To whom correspondence should be addressed. Tel.: +34 968 228284. Fax: +34 968 364147 or +34 968 363963. E-mail: neptuno@um.es.

§ Universidad de Murcia.

⊥ Universidad de Castilla-La Mancha.

[1] Abbreviations: AKP-C, basic heme peroxidase from artichoke (*Cynara scolymus* L.); ABTS, 2,2′-azino-bis(3-ethylbenzthiazoline-6-sulfonic acid); BP 1, barley grain peroxidase 1; Ca^{2+}, calcium ions; CD, circular dichroism; EDTA, ethylenediaminetetraacetic acid; H_2O_2, hydrogen peroxide; HRP, horseradish peroxidase; LiP, lignin peroxidase; PNP, cationic peanut peroxidase; 5cHS and 6cHS, penta- and hexacoordinate high-spin ferric heme iron, respectively.

10.1021/bi034580z CCC: $25.00
Published on Web 06/28/2003

by the polypeptide architecture (*25*) acting to restrict access or binding of the reducing substrate to the active site. Specificity is also modulated by factors including gene expression and protein targeting, so a particular peroxidase may not naturally come into contact with many potential substrates (*3*, *26*). The structures of several of the peroxidases from classes I, II, and III have been determined and found to share a number of features, including the overall protein fold, in particular the positions of various α-helices, and the general architecture of the heme pocket with the high-spin ferric iron coordinated to the proximal histidine and the conserved distal histidine and arginine residues that play important roles in compound I formation (*19*). Many peroxidases, especially those from classes II and III, also contain tightly bound structural metal ions (particularly calcium) and are glycosylated. The total mass of a monomeric peroxidase such as HRP is around 43 000 Da (*3*).

Artichoke peroxidase C (AKP-C) is a basic isoenzyme (p*I* > 9) which has been purified to homogeneity from artichoke flowers (*27*). AKP-C, as obtained from the plant, was characterized as a fairly typical class III peroxidase with good activity at neutral to acid pH toward phenolic substrates such as chlorogenic and caffeic acids, which are abundant in artichoke flowers. However, the UV−visible spectrum of native AKP-C exhibited a rather high Soret (404 nm) extinction coefficient of 137 000 ± 3000 M^{-1} cm^{-1}, and the peak was unusually sharp, lacking the shoulder at ∼380 nm characteristic of HRP. The resonance Raman spectrum of AKP-C indicated a majority 6-aquo hexacoordinate high-spin (6cHS) ferric iron species, compared to the more usual pentacoordinate (5cHS) iron seen in HRP and most other class III peroxidases. Additionally, the rate constant of compound I formation, k_1, of AKP-C was unusually low, at 7.4×10^5 M^{-1} s^{-1}.

Taken together, these data suggested that AKP-C might not be as typical as first thought. We have therefore carried out further spectroscopic and kinetic experiments to probe in more detail the reaction of AKP-C with H_2O_2 and, in particular, to examine the effect of calcium ions (Ca^{2+}) on reactivity. Both peroxidase and Ca^{2+} are known to be involved in regulating the concentrations of H_2O_2 and other active oxygen species in plant cells (*28*), so the data presented in this study on Ca^{2+}-dependent changes in the reactivity of AKP-C with H_2O_2 may reveal a way in which plants can adjust the activity of peroxidase in response to the environmental conditions. Furthermore, AKP-C is an abundant and easily purified enzyme with potential industrial and other applications. Controlling the rate of compound I formation could, in this respect, be of some importance.

MATERIALS AND METHODS

Artichoke Peroxidase C. AKP-C was purified from fresh artichoke (*Cynara scolymus* L.) flowers grown in Murcia (southeastern Spain), using the published procedure (*27*). The enzyme was extensively dialyzed against water, lyophilized, and stored at −20 °C. Artichokes are commercially cultivated in Murcia from November through June; we have carried out purifications and studies using material from different seasons and years and have found no evidence of variations in the enzyme. The purified AKP-C was homogeneous by SDS−PAGE stained with silver, was found to consist of a single isoenzyme with p*I* > 9 using isoelectric focusing, and exhibited an Rz ($A_{404\ nm}/A_{280\ nm}$) of 3.3−3.8 (dependent on the presence of calcium ions (Ca^{2+}) and/or ethylenediaminetetraacetic acid (EDTA), see below).

Chemicals. Reagent-grade H_2O_2 (30% v/v) was obtained from BDH-Merck (Poole, UK), and its concentration was determined spectrophotometrically using $\epsilon_{240\ nm} = 43.7$ M^{-1} cm^{-1}. All other chemicals were of reagent grade and obtained from Sigma or Aldrich (Madrid, Spain). Unless otherwise indicated, all experiments were performed in 50 mM tris(hydroxymethyl)aminomethane-HCl (Tris-HCl) buffer, pH 7.0, which did not form a precipitate in the presence of $CaCl_2$. All solutions were prepared using water drawn from a Milli-Q system (Millipore).

Electronic Absorption Spectroscopy. UV−visible electronic absorption spectra were recorded using a PC-controlled Perkin-Elmer Lambda 2 spectrophotometer at 25 °C (Haake D1G circulating water bath). Spectra of AKP-C as purified, in the presence of excess Ca^{2+}, and in the presence of excess EDTA were obtained. The dissociation constant (K_d) of AKP-C and Ca^{2+} was calculated from titrations of $CaCl_2$ with AKP-C, recording the spectrum after each addition. The end point was taken to have been reached when no further absorbance changes were observed, taking into account the dilution of the enzyme during the titration. A plot of the concentration of bound ligand divided by total ligand added against bound ligand ([EL]/[L_0] vs [EL]) due to Scatchard (*29*) gave a straight line with slope $-K_a$ ($-1/K_d$) and an intercept at the *x*-axis equal to the concentration of ligand binding sites (which for an enzyme with a single binding site is equal to the enzyme concentration). The alkaline transition of AKP-C in the presence of Ca^{2+} or EDTA was observed in 50 mM Tris-HCl at pH 7, 8, 9, 10, and 11. The spectra of AKP-C with Ca^{2+} or EDTA in a nonaqueous medium were obtained by preparing the samples in aqueous solution, followed by lyophilization and reconstitution in HPLC-grade methanol.

Rapid Kinetics. UV−visible rapid-mixing stopped-flow experiments were done on an Applied Photophysics Ltd. (Leatherhead, UK) Pi-Star 180 spectrometer with a stopped-flow unit at 25 °C (Neslab RTE-7 circulating water bath). For stopped-flow measurements, the apparatus was operated in single-mixing mode using the 1-cm-path-length observation cell and demonstrated a dead time of approximately 1.1 ms. The reactions of AKP-C with H_2O_2 were observed under pseudo-first-order conditions at 405 nm (for AKP-C as purified and with EDTA) or 398 nm (with added $CaCl_2$). Concentrations of the reagents are given in the Results and figures. The kinetic data were fitted to exponential functions using the PiStar 180's nonlinear regression curve-fitting program. The data points shown in the figures are the means of at least three (normally five) repeat observations. Formation of compounds I and II was also observed using multiwavelength kinetics that were analyzed globally using the Pro/K package (Applied Photophysics) to obtain the best-fit spectrum of each enzyme species.

Circular Dichroism Spectroscopy. Circular dichroism (CD) spectroscopy was also done on the Applied Photophysics Pi-Star 180 spectrometer with a thermostated (25 °C) and nitrogen-purged cuvette holder attached. Near-UV−visible CD spectra in the Soret region were obtained using a 1-cm-

path-length cuvette containing 15 μM AKP-C in 10 mM Tris-HCl buffer, pH 7, with 400 μM Ca^{2+} or 1 mM EDTA added. Similar far-UV spectra were obtained using a 1-mm path length and 1 μM enzyme.

RESULTS AND DISCUSSION

The Electronic Absorption Spectrum of AKP-C: Effects of Calcium Ions and EDTA. The UV−visible electronic absorption spectrum of AKP-C, as obtained from the plant, is unusual for a class III peroxidase and is highly reminiscent of the spectrum of lignin peroxidase (LiP) from class II (*30*). The Soret extinction coefficient of AKP-C has previously been determined, using the pyridine hemochrome method, to be $\epsilon_{404\,nm} = 137\,000 \pm 3000\ M^{-1}\ cm^{-1}$ (*27*). The Soret peak of AKP-C is, therefore, more intense and considerably sharper, lacking the shoulder at ~380 nm, than that of HRP-C ($\epsilon_{403\,nm} = 102\,000\ M^{-1}\ cm^{-1}$ (*9*)), which is the archetypal class III peroxidase. In a previous study (*27*), resonance Raman spectra indicated that AKP-C was a mixture of at least two ferric heme iron spin forms: a majority 6-aquo hexacoordinate high-spin (6cHS) species along with a pentacoordinate high-spin (5cHS) species. It should be noted that it is generally accepted that LiP is 6cHS and HRP-C is 5cHS.

Heme peroxidases of all classes contain metal ion binding sites, the metal ions generally serving to stabilize the polypeptide structure (*31*). To our knowledge, all class II and III peroxidases strongly bind calcium ions (Ca^{2+}) at conserved sites on the distal and proximal sides of the heme pocket (*8*, *32*). The only known exception is barley peroxidase, BP 1, which has a, so far, unique Ca^{2+} binding site with a rather low affinity for Ca^{2+} ($K_d = 4$ mM) that exerts conformational control over enzyme activity (*33*). Perhaps surprisingly, Ca^{2+} binding to BP 1 leaves its UV−visible spectrum virtually unchanged (*33*) but presents itself in the form of Ca^{2+}-dependent changes in kinetic behavior of the enzyme during compound I formation, changing from a slow reaction following H_2O_2-dependent saturation kinetics to a rapid nonsaturating reaction, that in some respects are similar to the results obtained for AKP-C (see below). In light of the unusual electronic absorption and resonance Raman spectra of AKP-C and the known importance of Ca^{2+} binding in peroxidase structure, we decided to examine the effects of these cations on AKP-C.

The addition of excess Ca^{2+} (50 μM) to the AKP-C sample (0.95 μM) caused the Soret extinction to fall to a value of $\epsilon_{405\,nm} = 114\,000 \pm 5000\ M^{-1}\ cm^{-1}$, more typical of a class III ferric peroxidase. The peak also broadened, forming a shoulder at ~380 nm (Figure 1). The addition of EDTA (500 μM) to AKP-C, either as purified or with previously added Ca^{2+}, caused the Soret maximum to rise ($\epsilon_{404\,nm} = 145\,000 \pm 4000\ M^{-1}\ cm^{-1}$) and the peak to sharpen (Figure 1). Other differences between the spectra of Ca^{2+}-free and Ca^{2+}-bound AKP-C were a shift of the peak at 499 nm to 493 nm with some loss of sharpness and a shift of the peak at 632 nm to 635 nm. These data suggested that AKP-C possesses a binding site from which Ca^{2+} can be removed comparatively easily and also that AKP-C, as purified from the plant, lacks its full complement of Ca^{2+}.

Dissociation Constant of Calcium Ions. The Scatchard plot of titrations of AKP-C with Ca^{2+} gave a straight line that

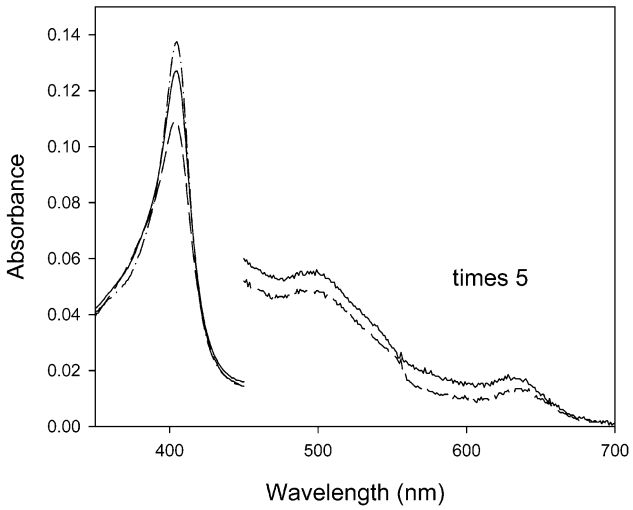

FIGURE 1: Electronic absorption spectra of artichoke peroxidase C (AKP-C, 0.95 μM) in 50 mM Tris-HCl, pH 7.0. Solid line, AKP-C as purified; dashed line, with $CaCl_2$ (50 μM); dot−dashed line, with ethylenediaminetetraacetic acid (500 μM). Expanded region (× 5) shows AKP-C as purified and with $CaCl_2$.

suggested that ligand binding was a simple noncooperative process, and yielded a dissociation constant, K_d, for Ca^{2+} of 17.8 ± 2.3 μM. The intercept at the *x*-axis (concentration of enzyme-bound ligand, [EL], at the end point) was equivalent to the AKP-C concentration used (2.08 μM), indicating that Ca^{2+} binding was being measured at a single site of the two which are presumably present in the enzyme, but without indicating which. The K_d for Ca^{2+} was approximately confirmed in peroxidase activity assays with 2,2′-azino-bis-(3-ethylbenzthiazoline-6-sulfonic acid) (ABTS, 2 mM; H_2O_2, 0.2 mM; AKP-C, 3.2 nM; measured at 414 nm using $\epsilon = 31\,100\ M^{-1}\ cm^{-1}$ for radical product, in 50 mM sodium citrate buffer, pH 4.5). The activity of AKP-C incubated with increasing concentrations of $CaCl_2$ rose approximately 3-fold between 0 and 1 mM Ca^{2+}, with the half-maximal increase in activity at approximately 50 μM Ca^{2+}, close to the titration K_d value. This result tends to suggest that Ca^{2+} binding affects the rate of reaction of compound II with reducing substrates (*34*) as well as the rate of compound I formation, as discussed below.

Ca^{2+} titrations of cationic peanut peroxidase (PNP), monitored using ^1H NMR, gave $K_d = 0.1$ μM for both binding sites (*35*), so it appears that the K_d of one of the Ca^{2+} in AKP-C was intermediate between the values for PNP and BP 1. In the case of HRP-C, Ca^{2+} could only be removed slowly from the enzyme using a combination of guanidinium hydrochloride and EDTA (*31*). However, EDTA alone was capable of rapidly removing Ca^{2+} from AKP-C, as shown by the UV−visible spectra. In fact, it was quite possible for the enzyme to go through various cycles of Ca^{2+} addition and removal without suffering greatly in activity or spectral terms.

Alkaline Transition of AKP-C. There were no changes observed in the absorbance spectrum of AKP-C over the pH range 4−10. The presence or absence of Ca^{2+} had a significant effect on the alkaline transition of ferric AKP-C between pH 10 and 11. Figure 2A shows that, in the presence of Ca^{2+}, the Soret peak was shifted from 405 to 412 nm and the 493 nm visible peak to around 550 nm. The peak at 635 nm was abolished. The changes were essentially reversible

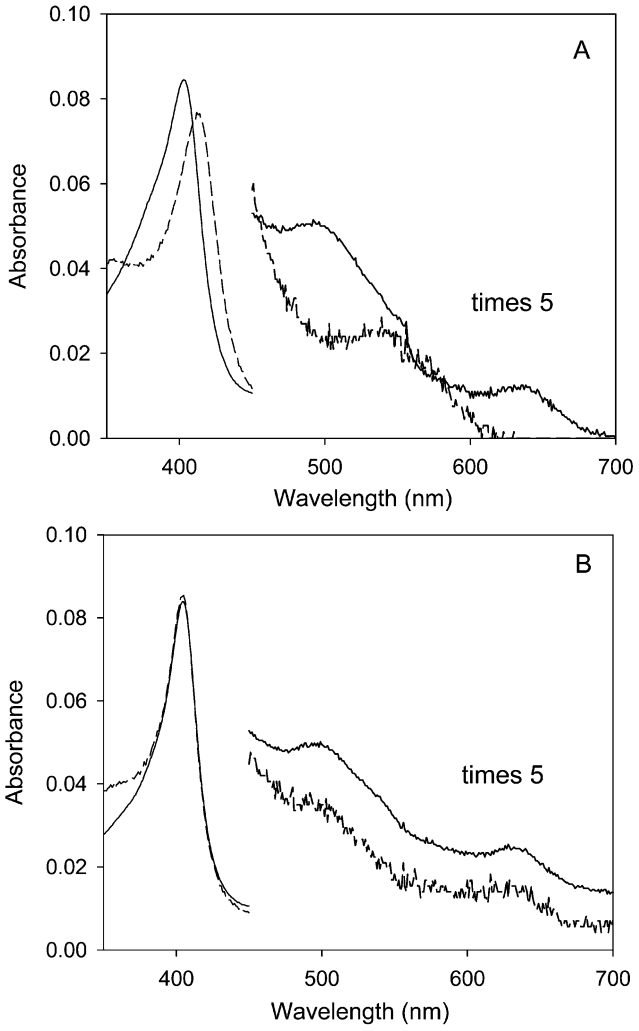

FIGURE 2: Alkaline transition (pH 10−11) of artichoke peroxidase C (AKP-C, ~0.6 μM) in the presence and in the absence of Ca^{2+}. (A) AKP-C with $CaCl_2$: solid line, pH 10; dashed line, pH 11. (B) AKP-C with ethylenediaminetetraacetic acid (no Ca^{2+}): solid line, pH 10; dashed line, pH 11. All spectra in 50 mM Tris buffer.

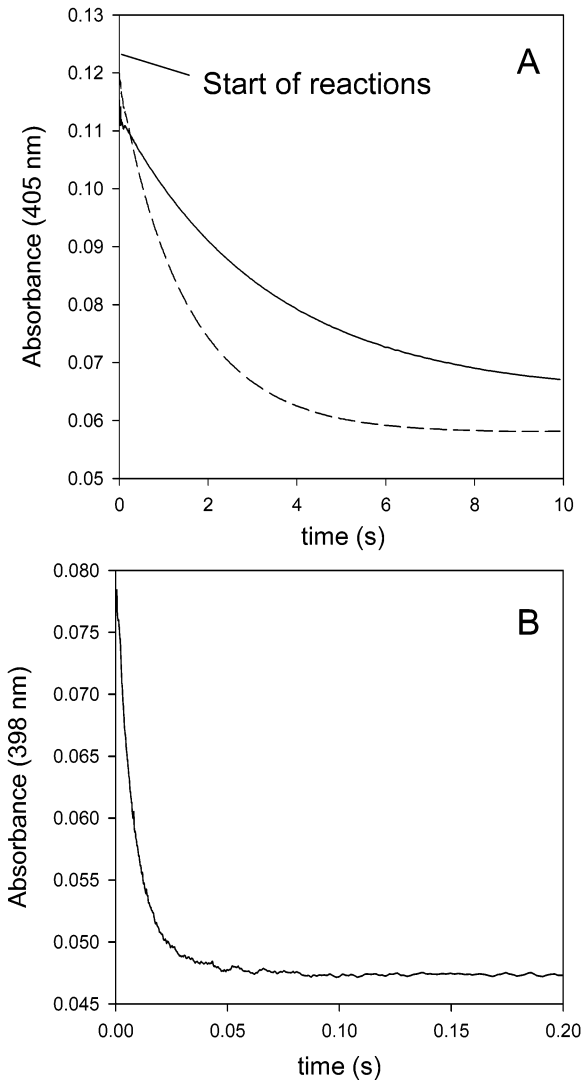

FIGURE 3: Stopped-flow kinetic traces of the reaction of artichoke peroxidase C (AKP-C) with hydrogen peroxide to form compound I. (A) Solid line, AKP-C as purified ([H_2O_2] = 12.5 μM) and dashed line, with ethylenediaminetetraacetic acid (EDTA) ([H_2O_2] = 25 μM). (B) AKP-C with $CaCl_2$ ([H_2O_2] = 5 μM). All experiments were done in 50 mM Tris-HCl, pH 7.0, [AKP-C] = 0.96 μM, [EDTA] = 5 mM, [$CaCl_2$] = 500 μM.

on lowering the pH. These data are consistent with hydroxyl ion or possibly bis-histidine coordination to the heme iron, although the second possibility seems less likely since the spectral changes are quite different from those previously observed in LiP (*36*). In Ca^{2+}-free AKP-C (with EDTA), changes between pH 10 and 11 were minimal (Figure 2B) and suggest that the coordination of the heme was unaltered, consistent with the presence of a ligand, presumably water, at the sixth coordination site of the iron or of other Ca^{2+}-dependent differences (e.g., conformational) that permit (with Ca^{2+}) or prohibit (without Ca^{2+}) hydroxyl ion coordination.

Effects of Calcium Ions and EDTA on the Formation of AKP-C Compound I. The apparent second-order rate constant for AKP-C compound I formation has previously been determined to be $k_1 = 7.4 \times 10^5$ M^{-1} s^{-1} (*27*), an unusually low value for a class III peroxidase since the k_1 values of most 5cHS peroxidases tend to be around $(1-2) \times 10^7$ M^{-1} s^{-1} (*3*). However, k_1 in the case of LiP compound I formation is 5.4×10^5 M^{-1} s^{-1} (*3*), rather closer to the value given above for AKP-C. These results can be rationalized if both LiP and AKP-C are taken to be, at least predominantly, 6cHS, due to the need to displace the 6-aquo ligand from the active site before H_2O_2 can bind to the iron center, initiating compound I formation. However, in light of the results presented above for the binding of Ca^{2+} to AKP-C, we decided to further examine the effects of Ca^{2+} on the reaction kinetics of AKP-C with H_2O_2 using stopped-flow.

AKP-C, as purified, demonstrated a biphasic reaction with H_2O_2 (Figure 3A), with approximately 25% of the total observed amplitude (absorbance fall) occurring in the fast phase and 75% in the slow. The stopped-flow data were therefore consistent with the resonance Raman spectra (*27*) that indicated the presence of at least two AKP-C species with distinct heme coordinations. Furthermore, assuming that the extinction changes for the reactions were of a roughly similar magnitude (which is reasonable, considering the spectra of the enzyme species and compound I), it appeared that the proportions of the reactions with H_2O_2 (the slow phase representing at least three-quarters of the total) agreed with the populations of 6cHS (slow phase) and 5cHS (fast phase) species in the enzyme sample. The rates of both phases were dependent on the H_2O_2 concentration. The faster

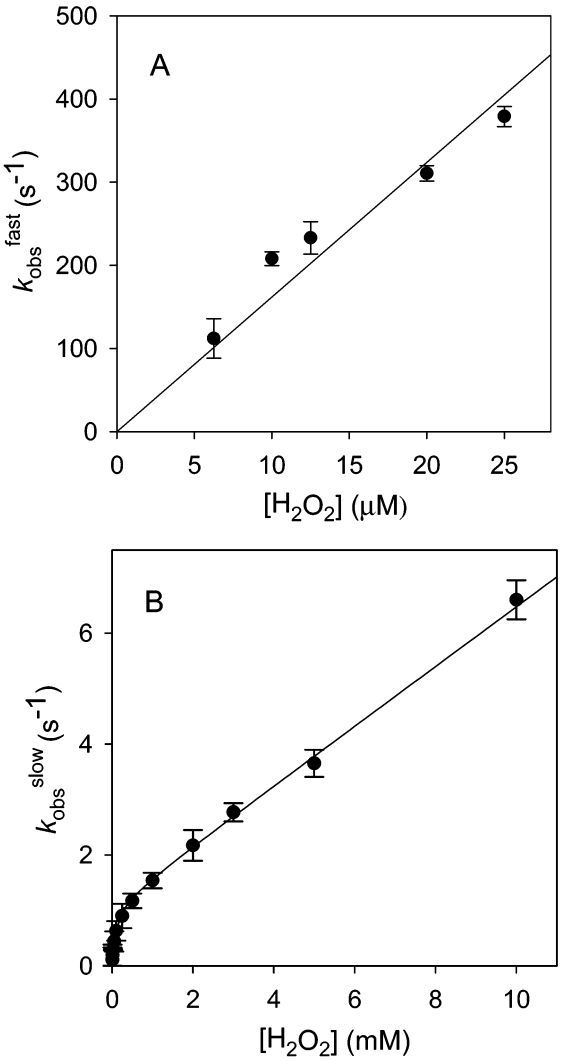

FIGURE 4: Second-order plots (observed rate constant, k_{obs}, versus hydrogen peroxide concentration, $[H_2O_2]$) for the two phases observed during the reaction of artichoke peroxidase C (AKP-C, as purified) with H_2O_2. (A) Fast phase, the slope of straight line fitted to the data yielded a second-order rate constant for compound I formation of $k_1 = 1.6 \times 10^7$ M^{-1} s^{-1}; this value was almost identical to the value obtained in the presence of $CaCl_2$. (B) Slow phase, using eq 4 and Appendix, the data gave $k_1' = 537$ M^{-1} s^{-1}; these data were essentially identical to those obtained in the presence of ethylenediaminetetraacetic acid.

reaction could be determined only at fairly low H_2O_2 concentrations (up to about 40 μM) before becoming too rapid to measure reliably; at higher concentrations its presence could be inferred from the "missing" amplitude at the start of observations (during the stopped-flow instrument's dead time). A plot (Figure 4A) of the observed rate constants for the fast reaction (k_{obs}^{fast}, s^{-1}) against $[H_2O_2]$ yielded an apparent second-order rate constant for the fast phase of $k_1^{fast,app} = 1.6 \times 10^7$ M^{-1} s^{-1}, which is a typical value for a peroxidase. The plot also passed through the origin, suggesting an irreversible reaction. The observed rates (k_{obs}^{slow}) of the slow phase were approximately 100-fold lower than those of the fast phase, and their dependence on H_2O_2 was more complex (Figure 4B). At lower $[H_2O_2]$, the second-order plot appeared hyperbolic but a maximum rate (V_{max}) was not reached, a linear relationship to $[H_2O_2]$ being observed at higher concentrations.

The addition of $CaCl_2$ (1 mM) to the enzyme sample had a profound effect on the stopped-flow observations. Under these conditions, the reaction with H_2O_2 consisted of a single fast phase with an amplitude equal to the sum of the fast and slow phases observed previously (Figure 3B), taking into account the lower extinction coefficient of Ca^{2+}-bound AKP-C. The second-order plot of k_{obs} gave a value of $k_1^{app} = 1.7 \times 10^7$ M^{-1} s^{-1}, in agreement with the value of the $k^{fast,app}$ above (the small difference most probably being due to the greater amplitude of the reaction in the presence of Ca^{2+} that facilitated more accurate measurements at higher H_2O_2 concentrations), suggesting that all the AKP-C was now reacting with H_2O_2 as a typical 5cHS peroxidase.

The addition of EDTA (5 mM) to the enzyme sample had the converse effect to $CaCl_2$: the fast phase was abolished and AKP-C reacted more slowly, with the complex H_2O_2-dependent behavior of the slow phase now dominant (Figures 3A and 4B). The effects of Ca^{2+} removal in AKP-C were markedly different from the effects that have been observed in HRP-C. The k_1 of HRP-C is not greatly affected by the removal of Ca^{2+}, dropping only slightly to 1.4×10^7 M^{-1} s^{-1} (*31*), suggesting that Ca^{2+} may possibly play a more intimate role in controlling AKP-C activity than is the case for HRP-C. Mutation of Glu64 in the distal Ca^{2+} binding site of HRP-C did result in a large reduction of k_1 to 4.3×10^5 M^{-1} s^{-1} (*31*), and one of the ligands to the proximal Ca^{2+} (Thr171) is adjacent to the proximal histidine (His170), so changes to this residue may possibly also affect enzyme reactivity.

The circular dichroism (CD) spectrum of AKP-C (data not shown) was similar to that of HRP-C (*37*), with a peak at ~410 nm in the Soret and a double trough at 222 and 208 nm in the far-UV. The spectra were essentially identical in the presence or absence (with EDTA) of Ca^{2+}, indicating that Ca^{2+} binding does not lead to major conformational changes in the protein secondary (far-UV CD) or tertiary (Soret CD) structures. Since, at present, neither the full amino acid sequence nor the crystal structure of AKP-C is available, it is not possible to do more than speculate about any differences between the Ca^{2+} binding sites of AKP-C and HRP-C or the nature of any changes that occur in the structure of the enzyme upon Ca^{2+} binding, except that, taking into account the CD data, they will be subtle in nature. It is worth noting, however, that resonance Raman spectra of HRP-C from which the proximal Ca^{2+} has been removed (*38*) bear some similarity to the data for AKP-C.

Ca^{2+} binding in AKP-C is, therefore, somewhat enigmatic since in some ways it is more akin to HRP-C and in others to BP 1. Despite the very significant effects of Ca^{2+} binding to BP 1 on the kinetics of compound I formation, the UV−visible spectrum was almost unaltered, showing that the Ca^{2+} did not perturb the heme iron coordination or spin state. The crystal structure of BP 1 indicates that the distal histidine is mobile, turning away from the iron in the inactive enzyme (pH > 5) and reorienting into position above the heme in a proton-induced conformational change in the slow reacting form of BP 1 ($k_{cat}^{app} = 4.5$ s^{-1} at pH 3.1) (*33*, *39*). Ca^{2+} binding, possibly in a novel distal site, presumably leads to further conformational changes and/or stabilizes the histidine or other groups in fast-reacting BP 1 ($k_1 = 1.5 \times$

Scheme 1: Mechanism of Reaction of Ca^{2+}-Bound Artichoke Peroxidase C (Ca^{2+}−E) with Hydrogen Peroxide (H_2O_2)[a]

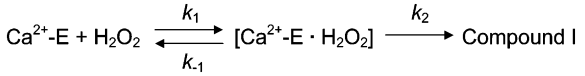

[a] The mechanism will exhibit single-exponential nonsaturating kinetic behavior in the stopped-flow if k_2 is too fast to be observed (eqs 1 and 2).

10^7 M^{-1} s^{-1}) (*33*). The conformational change of BP 1 is fairly slow, whereas stopped-flow experiments with AKP-C (data not shown) suggested that the changes (e.g., to the absorption spectrum) caused by Ca^{2+} binding occur rapidly, i.e., beyond the stopped-flow observation limit under pseudo-first-order conditions and possibly diffusion-controlled.

Stability of Compound I. AKP-C compound I was observed to be unstable compared to that of HRP-C, decaying to compound II in less than 1 min. The addition of Ca^{2+} did not affect the rate of compound II formation ($k_{obs} \approx 0.1-0.4$ s^{-1}), which was slightly dependent on [H_2O_2]. At higher (~10 mM) H_2O_2 concentrations, the formation of compound III (due to the binding of H_2O_2 to compound II) was also observed, which may have affected the observed rates of compound II formation, resulting in the small range of k_{obs} values observed, whereas compound II formation itself is independent of [H_2O_2]. Multiwavelength kinetic data allowed the spectrum of compound I to be observed, proving to be typical, with a slightly blue-shifted and much less intense ($\epsilon_{400\,nm} \approx 60\,000$ M^{-1} cm^{-1}) Soret peak compared to the ferric enzyme (*27*). AKP-C compound II also exhibited a typical absorbance spectrum, with an intense red-shifted Soret peak.

The similarity of the rates of decay of compound I to compound II in samples that contained Ca^{2+} and those that did not suggested that the compound I formed in each case was identical, unlike the case of ascorbate peroxidase, in which two distinct compound I species have been identified (*16*).

Kinetic Analysis and Mechanisms of Compound I Formation in AKP-C. (a) Compound I Formation in the Presence of Calcium Ions. As observed in the spectrophotometric assays described above, Ca^{2+} produces a change in AKP-C, favoring the presence of a Ca^{2+}−AKP-C species with a typical 5cHS spectrum. Stopped-flow experiments suggested that all the AKP-C was reacting with H_2O_2 as a typical peroxidase (Figures 3B and 4A). Although no evidence for a two-step reaction was observed, it is widely accepted that peroxidases follow such a mechanism during compound I formation (*17*−*20*). Thus, in the presence of Ca^{2+}, the mechanism of AKP-C compound I formation can be depicted as shown in Scheme 1, where Ca^{2+}−E represents Ca^{2+}-bound AKP-C.

This mechanism predicts biexponential behavior, with the second phase (controlled by k_2) being faster than the first (controlled by k_1[H_2O_2]) in the range of peroxide concentrations used for this experiment. Although the value of k_2 for Ca^{2+}−E has not been determined, the nonsaturating kinetic behavior of the enzyme suggests that this value is probably close to those of other peroxidases: approximately 2×10^3 s^{-1}, as determined for HRP-C using steady-state kinetics (*34*). The mechanism shown in Scheme 1, in which the first step is significantly slower than the second, has been kinetically

Scheme 2: Reaction Mechanism of Peroxidase with Hydrogen Peroxide (H_2O_2) Where the Enzyme Is an Equilibrium between a Reactive Form, E, and a Nonreactive Form, E*[a]

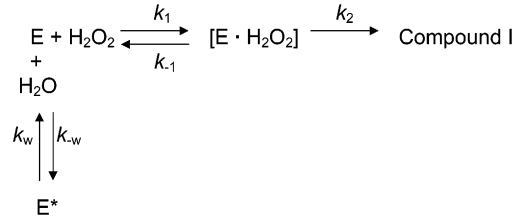

[a] The mechanism would give H_2O_2 concentration-dependent saturation kinetics (eq 3).

Scheme 3: Reaction Mechanism of Peroxidase with Hydrogen Peroxide (H_2O_2) Where the Enzyme Is an Equilibrium between Two Forms, E and E*, That React with H_2O_2 at Different Rates[a]

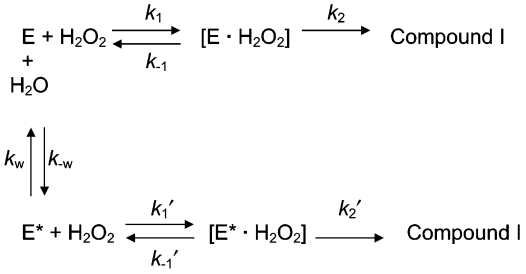

[a] Artichoke peroxidase C is proposed to follow such a mechanism in the absence of Ca^{2+} (eq 4 and Appendix).

resolved (*40*), with the values of the exponential phases given by

$$k_{fast} = k_2 \quad (1)$$

$$k_{slow} = k_1[H_2O_2] + k_{-1} \quad (2)$$

Therefore, for a peroxidase mechanism in which k_2 is greater than the stopped-flow limit (~500−600 s^{-1}), a single-exponential phase (the slower) is observed, and a linear dependence of the observed rate constant versus peroxide concentration is predicted. This is the behavior observed for the reaction of Ca^{2+}−E with H_2O_2. The second-order plot of k_{obs} gave a value of $k_1^{app} = 1.7 \times 10^7$ M^{-1} s^{-1}, similar to the value for reaction of other peroxidases, such as HRP-C or ascorbate peroxidase, with H_2O_2.

(b) Compound I Formation in the Presence of EDTA. Addition of EDTA to AKP-C efficiently chelates the Ca^{2+} from Ca^{2+}−AKP-C, as can be deduced from the UV−visible spectrum, and the abolition of the fast phase in purified AKP-C. EDTA increases the amount of the 6cHS form of AKP-C. The coordination of the heme has important consequences for the reactivity of the enzyme with H_2O_2. The apparent bimolecular rate constants (k_1) of compound I formation in most 5cHS peroxidases tend to be around $(1-2) \times 10^7$ M^{-1} s^{-1} (*3*). However, the rate constant for compound I formation in a typical 6-aquo 6cHS enzyme, such as LiP, drops to 5.4×10^5 M^{-1} s^{-1} (*3*). Two mechanisms for the reaction of water-coordinated peroxidases, involving displacement of the water molecule, are depicted in Schemes 2 and 3. The main difference between the mechanisms is that, in Scheme 2, the peroxide can react only with the 5cHS form, whereas in Scheme 3, both enzymatic forms are reactive toward the peroxide substrate.

Table 1: Rate Constants Controlling the Reaction of AKP-C with H_2O_2 To Form Compound I

k_1[a] (M^{-1} s^{-1})	k_1'[b] (M^{-1} s^{-1})	k_w[b] (s^{-1})	k_{-w}[b]
1.6×10^7	537	1.11	1424 (apparent,[c] s^{-1}) 25.7 (2nd order,[c] M^{-1} s^{-1})

[a] Determined from the slope of the straight line fitted to the data in Figure 4A. [b] Calculated using the data in Figure 4B and eq 4. [c] The apparent value of k_{-w} is divided by the concentration of water (55.5 M) to obtain the second-order constant, i.e., $k_{-w}^{app} = k_{-w}[H_2O]$.

A complete analysis of a simplified form of Scheme 2, in which it is assumed that the reaction controlled by k_2 is too fast to be observed using stopped-flow, gives the following expression for the slow phase (*33*):

$$k_{obs} = k_w[H_2O_2]/(k_w + k_{-w}/k_1 + [H_2O_2]) \quad (3)$$

The observed kinetics of the slow reaction are predicted to show saturation with respect to the H_2O_2 concentration.

Because the experimental data for the reaction of AKP-C with H_2O_2 in the presence of EDTA revealed more complex behavior (identical to the data shown in Figure 4B), we proceeded to a detailed kinetic analysis of the mechanism presented in Scheme 3 (see Appendix). Assuming that the first-order steps, controlled by k_2 and k_2', are much faster than the other steps, the dependence of the slow phase on H_2O_2 concentration followed a 2:1 expression:

$$k_{obs} = \frac{k_1'[H_2O_2]^2 + ((k_1k_w + k_1'k_{-w})/k_1)[H_2O_2]}{[H_2O_2] + (k_w + k_{-w}/k_1)} \quad (4)$$

The data presented in Figure 4B fitted eq 4, and the values for k_1', k_w, and k_{-w} could be determined assuming a value for k_1 of 1.6×10^7 M^{-1} s^{-1} (Table 1). According to the mechanism described in Scheme 3, AKP-C in the presence of EDTA is an equilibrium between two forms, a slow-reacting 6-aquo 6cHS form (E*) and a fast-reacting 5cHS form (E). In water solution ($[H_2O] = 55.5$ M), the equilibrium is almost completely displaced to E* ($K_w = k_{-w}/k_w$), and also gives an apparent value of k_{-w}, where $k_{-w}^{app} = k_{-w}[H_2O]$, as shown in Table 1. Addition of H_2O_2 displaces the equilibrium to form E, particularly at higher H_2O_2 concentrations, resulting in the transition from saturating to nonsaturating kinetics. It should be noted that form E, posited here, is not necessarily identical to the 5cHS Ca^{2+}-bound form of AKP-C (Ca^{2+}−E). The spectra of AKP-C with Ca^{2+} or EDTA, prepared in aqueous solution but then lyophilized and redissolved in methanol so that the sixth coordination position to the iron should be vacant (i.e., 5cHS) in both samples, were distinct (Figure 5). In Ca^{2+}-free AKP-C, the Soret peak was shifted to 397 nm, compared to 398 nm with Ca^{2+}; Ca^{2+}-bound AKP-C also exhibited small peaks at ~380 and ~600 nm that were not present with EDTA. The distinct spectra in the presence and in the absence of Ca^{2+} suggest the existence of two pentacoordinate forms of AKP-C, one of these being form E and the other Ca^{2+}−E. A detailed examination of the resonance Raman data (*27*) also hinted at the presence of a second 5cHS or possibly an unusual 6c quantum mechanically mixed-spin species, which has also been suggested to be present in HRP-C from which the proximal Ca^{2+} has been removed

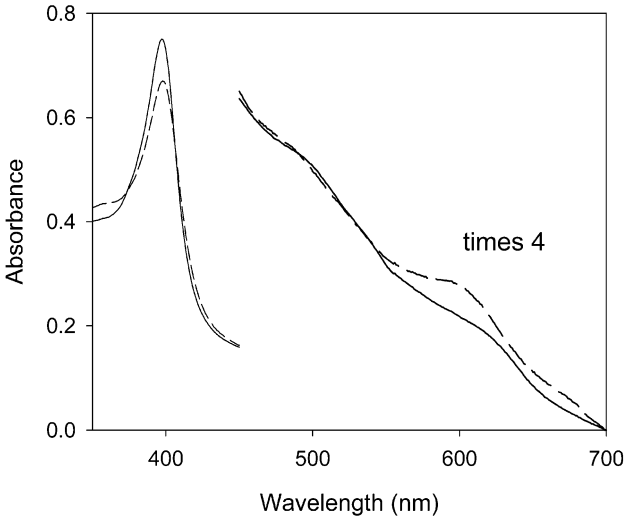

FIGURE 5: Electronic absorption spectra of artichoke peroxidase C (AKP-C) in methanol. Solid line, sample prepared in the presence of ethylenediaminetetraacetic acid (EDTA, no Ca^{2+}); dashed line, sample prepared with $CaCl_2$. (AKP-C (~0.5 μM) was mixed with 500 μM EDTA or 50 μM $CaCl_2$ in 10 mM Tris-HCl, pH 7.0. The samples were then lyophilized to dryness and reconstituted in HPLC-grade methanol.

(*38*). The possibility also needs to be considered that the rates of reaction with H_2O_2 (k_1) of Ca^{2+}−E and E may not be identical, which could affect the kinetic analysis somewhat.

(c) Compound I Formation in AKPC, As Extracted from the Plant. The spectroscopic evidence suggests that AKP-C, purified from artichoke, consists of a mixture of species: Ca^{2+}-bound 5cHS (Ca^{2+}−E) and 6-aquo 6cHS (E*) in equilibrium with a small amount of Ca^{2+}-free 5cHS (E). During reaction with H_2O_2, the kinetics followed by these species are distinct, as indicated in the previous sections. The rates of reaction of Ca^{2+}−AKP-C and 6-aquo AKP-C with H_2O_2 are sufficiently different that they can effectively be determined separately using stopped-flow and the proportions of the species determined from the amplitudes of the exponential curves. Ca^{2+}-free 5cHS AKP-C is a minor constituent of the enzyme sample in aqueous solution but becomes significant at higher H_2O_2 concentrations when it affects the kinetics of the reaction of 6-aquo AKP-C. The compound I formed by the reaction of each species appears to be identical and, from its UV−visible absorption spectrum, is an oxyferryl (Fe(IV)═O) π-cation radical species, as found in HRP-C (*14*) and most, if not all (*21*), other class III peroxidases. AKP-C compound I formed in the presence and in the absence of Ca^{2+} also decays to compound II at the same rate and will form compound III with excess H_2O_2.

CONCLUSIONS

This study has clearly demonstrated the importance of heme coordination in the reactivity of peroxidase with its natural substrate, H_2O_2. Coordination of a water molecule at the sixth coordination position of the ferric iron center of AKP-C produced a drastic change in the velocity of compound I formation. The rate constant (k_1) dropped from 1.6×10^7 to 5.4×10^2 M^{-1} s^{-1}; a difference of more than 5 orders of magnitude. Ca^{2+} effectively controlled the heme

iron coordination and hence the rate of reaction. Although a more detailed physiological study would be required, the data indicate the potential importance of heme coordination in the regulation of peroxidase activity in vivo, and in this respect it is worth noting that Ca^{2+} has already been shown to be implicated in H_2O_2 homeostasis, cell signaling, and pathogen defense in plants in pathways linked to catalase (*41*) and peroxidase (*28*). We expect that further studies on AKP-C will show that it is distinct in various ways but also shares many properties in common with other peroxidases, such as a catalase-like reaction and mechanism-based (suicide) inactivation with peroxides (*42*−*46*). Whatever the results of future experiments, it is clear that the Ca^{2+} concentration and the coordination state of the heme iron will need to be taken into careful consideration.

APPENDIX

Given herein is a kinetic analysis of the reaction of AKP-C with H_2O_2 in the absence of calcium ions, as shown in Scheme 3 (slow phase of the reaction of AKP-C, as purified, or the whole reaction in the presence of ethylenediaminetetraacetic acid).

Notation. X_1, X_2, X_3, concentrations of the species 6-aquo 6cHS AKP-C (E*), 5cHS AKP-C (E), and compound I (CI), respectively; $[S]_0$, initial concentration of H_2O_2; X_1^0, initial concentration of E*; X_2^0, initial concentration of E; $[E]_0$, total initial concentration of the enzyme, that is,

$$[E]_0 = X_1^0 + X_2^0 \tag{A1}$$

K_w, equilibrium constant for the interconversion of E* and E, that is,

$$K_w = k_{-w}/k_w \tag{A2}$$

Initial Conditions. (a) Initially the enzymatic forms E* and E are at equilibrium, with the sum of their concentrations being $[E]_0$ and the equilibrium constant being K_w (eq A2). Thus, the concentrations of E* and E are

$$X_1^0 = \frac{K_w[E]_0}{1 + K_w} \tag{A3}$$

$$X_2^0 = \frac{[E]_0}{1 + K_w} \tag{A4}$$

(b) CI is not present.

(c) The addition of H_2O_2 (S) disrupts the equilibrium between E* and E.

(d) The initial H_2O_2 concentration is much greater than that of the enzyme, that is,

$$[S]_0 \gg [E]_0 \tag{A5}$$

ensuring that the H_2O_2 concentration does not vary significantly during the reaction:

$$[S] \approx [S]_0 \tag{A6}$$

and all the interconversions between the enzymatic forms E, E*, ES, E*S, and CI are first-order or pseudo-first-order.

Scheme 4: Simplified Reaction Mechanism of Peroxidase with Hydrogen Peroxide (H_2O_2) Where the Enzyme Is an Equilibrium between Two Forms, E and E*, That React with H_2O_2 at Different Rates[a]

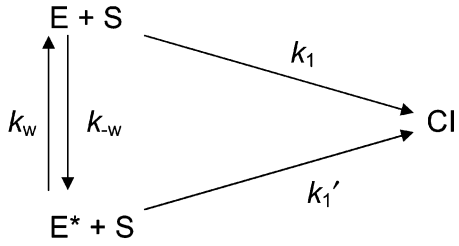

[a] The mechanism is a simplified version of Scheme 3.

Scheme 5: Connectivity Diagram for the Linear Compartmental System Equivalent to the Reaction Mechanism of Peroxidase with Hydrogen Peroxide Shown in Scheme 4[a]

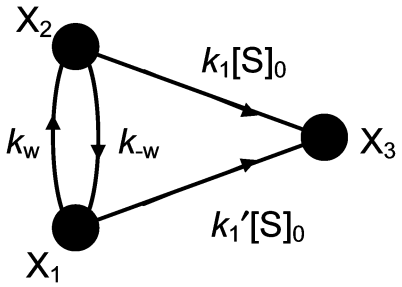

[a] The compartments X_1, X_2, and X_3 represent the species E*, E, and CI, respectively.

Time Equations for [E], [E], and [CI].* The equations for the accumulation of E*, E, and CI over time can be resolved from the linear system of differential equations that describe the kinetics of the reaction mechanism shown in Scheme 4, which is a simplified version of Scheme 3. The time equations can also be obtained by treating the enzyme mechanism as a linear compartmental system and directly applying the general equations recently developed for this type of system by García-Meseguer et al. (*47*) using the software that is described in this reference. The species E*, E, and CI were arbitrarily assigned to compartments (X_1, X_2, and X_3, respectively), and using one of the examples given in ref *47*, a connectivity diagram (Scheme 5) for the linear compartmental system equivalent to Scheme 4 was established.

In this way, it is possible to establish that

$$X_1 = A_{1,1}\, e^{-\lambda_1 t} + A_{1,2}\, e^{-\lambda_2 t} \tag{A7}$$

$$X_2 = A_{2,1}\, e^{-\lambda_1 t} + A_{2,2}\, e^{-\lambda_2 t} \tag{A8}$$

$$X_3 = A_{3,0} + A_{3,1}\, e^{-\lambda_1 t} + A_{3,2}\, e^{-\lambda_2 t} \tag{A9}$$

where λ_1 and λ_2 are the roots of the equation

$$\lambda^2 - F_1\lambda + F_2 = 0 \tag{A10}$$

and

$$F_1 = (k_1' + k_1)[S]_0 + k_w + k_{-w} \tag{A11}$$

$$F_2 = k_1'k_1[S]_0^2 + (k_1k_w + k_1'k_{-w})[S]_0 \tag{A12}$$

The equation roots (λ_1 and λ_2) are positive real numbers or complex numbers with the real part taking a positive value and satisfy the relationships

$$\lambda_1 + \lambda_2 = F_1 \tag{A13}$$

$$\lambda_1\lambda_2 = F_2 \tag{A14}$$

Their individual expressions are

$$\lambda_1 = \frac{F_1 - \sqrt{F_1^{\,2} - 4F_2}}{2} \tag{A15}$$

$$\lambda_2 = \frac{F_1 + \sqrt{F_1^{\,2} - 4F_2}}{2} \tag{A16}$$

The coefficients in eqs A7−A9 are given by

$$A_{1,1} = \frac{X_1^0(-\lambda_1 + k_{-w} + k_1[S]_0) + X_2^0 k_{-w}}{\lambda_2 - \lambda_1} \tag{A17}$$

$$A_{1,2} = \frac{X_1^0(-\lambda_2 + k_{-w} + k_1[S]_0) + X_2^0 k_{-w}}{\lambda_1 - \lambda_2} \tag{A18}$$

$$A_{2,1} = \frac{X_1^0 k_w + X_2^0(-\lambda_1 + k_1'[S]_0 + k_{-w})}{\lambda_2 - \lambda_1} \tag{A19}$$

$$A_{2,2} = \frac{X_1^0 k_w + X_2^0(-\lambda_2 + k_1'[S]_0 + k_{-w})}{\lambda_1 - \lambda_2} \tag{A20}$$

$$A_{3,0} = X_1^0 + X_2^0 \tag{A21}$$

and, finally

$$A_{3,1} = \frac{X_1^0(-k_1'[S]_0\lambda_1 + F_2) + X_2^0(-k_1[S]_0\lambda_1 + F_2)}{\lambda_1(\lambda_2 - \lambda_1)} \tag{A22}$$

$$A_{3,2} = \frac{X_1^0(-k_1'[S]_0\lambda_2 + F_2) + X_2^0(-k_1[S]_0\lambda_2 + F_2)}{\lambda_2(\lambda_1 - \lambda_2)} \tag{A23}$$

Equations A7−A9 and A15−A23 describe the changes over time of each of the enzymatic forms involved in the mechanism shown in Scheme 4. If X_1^0 and X_2^0 in these equations are substituted by the expressions given in eqs A3 and A4, they will then be a function of the total initial enzyme concentration, $[E]_0$, and the equilibrium constant, K_w, as well as the individual rate constants.

Single-Exponential Behavior. Equations A7−A9 contain two exponential terms; however, in practice, in many cases and specifically the case under consideration here—the reaction of AKP-C with H_2O_2 in the absence of Ca^{2+} (Schemes 3 and 4)—the time-dependent concentration variations of the enzymatic species involved in the reaction fit well to a single-exponential curve. Thus, the following section justifies the monoexponential behavior observed that implies that, in eqs A7−A9, the exponential term $A_{i,2}\, e^{\lambda_2 t}$, where $i = 1, 2, 3$, can be disregarded, reducing the equations to

$$X_1 = A_{1,1}\, e^{-\lambda_1 t} \tag{A24}$$

$$X_2 = A_{2,1}\, e^{-\lambda_1 t} \tag{A25}$$

$$X_3 = A_{3,0} + A_{3,1}\, e^{-\lambda_1 t} \tag{A26}$$

The necessary and sufficient condition for the exponential term to be disregarded is that the absolute value of λ_2 be much greater than that of λ_1:

$$\lambda_2 \gg \lambda_1 \tag{A27}$$

or, compared to the value of λ_1,

$$\lambda_2 \rightarrow \infty \tag{A28}$$

The consequences of eqs A27 and A28 are that

$$\lambda_2 - \lambda_1 \approx \lambda_2 \tag{A29}$$

and

$$\lambda_2 + \lambda_1 \approx \lambda_2 \tag{A30}$$

Taking into account eq A27 in eq A13, we obtain

$$\lambda_2 \approx F_1 \tag{A31}$$

If now eq A31 is applied to eq A14, the result is

$$\lambda_1 \approx F_2/F_1 \tag{A32}$$

The coefficients $A_{i,1}$ ($i = 1, 2, 3$) in eqs A24−A26 are described in eqs A17−A23. But taking into account eqs A11, A13, A28, and A29 and defining, for the sake of convenience, λ_1 as λ, the results for eqs A24−A26 are

$$X_1 = X_1^0\, e^{-\lambda t} \tag{A33}$$

$$X_2 = X_2^0\, e^{-\lambda t} \tag{A34}$$

$$X_3 = [E]_0(1 - e^{-\lambda t}) \tag{A35}$$

where λ, in agreement with eqs A32, A13, and A14, is given by

$$\lambda = \frac{a[S]_0^2 + b[S]_0}{c[S]_0 + d} \tag{A36}$$

where

$$a = k_1'k_1 \tag{A37}$$

$$b = k_1k_w + k_1'k_{-w} \tag{A38}$$

$$c = k_1' + k_1 \tag{A39}$$

$$d = k_w + k_{-w} \tag{A40}$$

Assuming that $k_1 \gg k_1'$, then $c \approx k_1$, and eq A36 can be simplified to give eq 4 (main text).

REFERENCES

1. Welinder, K. G. (1985) *Eur. J. Biochem. 151*, 497−450.
2. Welinder, K. G. (1992) *Curr. Opin. Struct. Biol. 2*, 388−393.

3. Dunford, H. B. (1999) *Heme Peroxidases*, Wiley-VCH, New York.
4. Obinger, C., Regelsberger, G., Pircher, A., Sevcik-Klöckler, A., Strasser, G., and Peschek, G. A. (1999) in *The Phototrophic Prokaryotes* (Peschek, G. A., et al., Eds.) pp 719−731, Kluwer Academic/Plenum Publishers, New York.
5. Welinder, K. G. (1991) *Biochim. Biophys. Acta 1080*, 215−220.
6. Asada, K. (1992) *Physiol. Plant. 85*, 235−241.
7. Kjalke, M., Andersen, M. B., Schneider, P., Christensen, B., Schülein, M., and Welinder, K. G. (1992) *Biochim. Biophys. Acta 1120*, 248−256.
8. Poulos, T. L., Edwards, S. L., Wariishi, H., and Gold, M. H. (1993) *J. Biol. Chem. 268*, 4429−4440.
9. Dunford, H. B., and Stillman, J. S. (1976) *Coord. Chem. Rev. 19*, 187−251.
10. Veitch, N. C., and Smith, A. T. (2001) *Adv. Inorg. Chem 51*, 107−162.
11. Van der Mijnsbrugge, K., Meyermans, H., van Montagu, M., Bauw, G., and Boerjan, W. (2000) *Planta 210*, 589−598.
12. Potikha, T. S., Collins, C. C., Johnson, D. I., Delmer, D. P., and Levine, A. (1999) *Plant Physiol. 119*, 849−858.
13. Mittler, R., Hallak Herr, E., Larus Orvar, B., van Camp, W., Willekens, H., Inzé, D., and Ellis, B. E. (1999) *Proc. Natl. Acad. Sci. U.S.A. 96*, 14165−14170.
14. Dolphin, D., Forman, A., Borg, D. C., Fajer, J., and Felton, R. H. (1971) *Rec. Res. Dev. Agric. Food Chem. 68*, 614−618.
15. Goodin, D. B., Mauk, A. G., and Smith, M. (1987) *J. Biol. Chem. 262*, 7719−7724.
16. Hiner, A. N. P., Martínez, J. I., Arnao, M. B., Acosta, M., Turner, D. D., Raven, E. L., and Rodríguez-López, J. N. (2001) *Eur. J. Biochem. 268*, 3091−3098.
17. Baek, H. K., and Van Wart, H. E. (1992) *J. Am. Chem. Soc. 114*, 718−725.
18. Rodríguez-López, J. N., Smith, A. T., and Thorneley, R. N. F. (1996) *J. Biol. Chem. 271*, 4023−4030.
19. Rodríguez-López, J. N., Lowe, D. L., Hernández-Ruiz, J., Hiner, A. N. P., García-Cánovas, F., and Thorneley, R. N. F. (2001) *J. Am. Chem. Soc. 123*, 11838−11847.
20. Hiner, A. N. P., Raven, E. L., Thorneley, R. N. F., García-Cánovas, F., and Rodríguez-López, J. N. (2002) *J. Inorg. Biochem. 91*, 27−34.
21. Converso, D. A. and Fernández, M. E. (1998) *Arch. Biochem. Biophys. 357*, 22−26.
22. Pappa, H., Patterson, W. R., and Poulos, T. L. (1996) *J. Biol. Inorg.Chem. 1*, 61−66.
23. Patterson, W. R., Poulos, T. L., and Goodin, D. B. (1995) *Biochemistry 34*, 4342−4345.
24. Morimoto, A., Tanaka, M., Takahashi, S., Ishimori, K., Hori, H., and Morishima, I. (1998) *J. Biol. Chem. 273*, 14753−14760.
25. Ator, M. A., and Ortiz de Montellano, P. R. (1987) *J. Biol. Chem. 262*, 1542−1551.
26. Welinder, K. G., Jespersen, H. M., Kjaersgard, I. V. H., Ostergaard, L., Abelskov, A. K., Hansen, L. N., and Rasmussen, S. K. (1996) in *Plant Peroxidases*: *Biochemistry and Physiology* (Obinger, C., Burner, U., Ebermann, R., Penel, C., and Greppin, H., Eds.) pp 173−178, University of Geneva, Geneva.
27. López-Molina, D., Heering, H. A., Smuevich, G., Tudela, J., Thorneley, R. N. F., García-Cánovas, F., and Rodríguez-López, J. N. (2003) *J. Inorg. Biochem. 94*, 243−254.
28. Kawano, T., and Muto, S. (2000) *J. Exp. Bot. 51*, 685−693.
29. Palmer, T. (1991) *Understanding Enzymes*, Ellis Horwood Ltd., Chishester, UK.
30. Nie, G., and Aust, S. D. (1997) *Biochemistry 36*, 5113−5119.
31. Shiro, Y., Kurono, M., and Morishima, I. (1986) *J. Biol. Chem. 261*, 9382−9390.
32. Gajhede, M., Schuller, D. J., Henriksen, A., Smith, A. T., and Poulos, T. L. (1997) *Nat. Struct. Biol. 4*, 1032−1038.
33. Rasmussen, C. B., Hiner, A. N. P., Smith, A. T., and Welinder, K. G. (1998) *J. Biol. Chem. 273*, 2232−2240.
34. Rodríguez-López, J. N., Gilabert, M. A., Tudela, J., Thorneley, R. N. F., and García-Cánovas, F. (2000) *Biochemistry 39*, 13201−13209.
35. Barber, K. R., Rodrígues-Morañón, M. J., Shaw, G. S., and van Huystee, R. B. (2003) *Eur. J. Biochem. 232*, 825−833.
36. George, S. J., Kvaratskhelia, M., Dilworth, M. J., and Thorneley, R. N. F. (1999) *Biochem. J. 344*, 237−244.
37. Pina, D. G., Shnyrova, A. V., Gavilanes, F., Rodríguez, A., Leal, F., Roig, M. G., Sakharov, I. Y., Zhadan, G. G., Villar, E., and Shnyrov, V. L. (2001) *Eur. J. Biochem. 268*, 120−126.
38. Howes, B. D., Feis, A., Raimondi, L., and Indiani, C. (2001) *J. Biol. Chem. 276*, 40704−40711.
39. Henriksen, A., Welinder, K. G., and Gajhede, M. (1997) *J. Biol. Chem. 273*, 2241−2248.
40. Hiromi, K. (1979) *Kinetics of Fast Enzyme Reactions—Theory and Practice*, John Wiley & Sons, New York.
41. Yang, T., and Poovaiah, B. W. (2002) *Proc. Natl. Acad. Sci. U.S.A. 99*, 4097−4102.
42. Arnao, M. B., Acosta, M., del Rio, J. A., Varón, R., and García-Cánovas, F. (1990) *Biochim. Biophys. Acta 1041*, 43−47.
43. Rodríguez-López, J. N., Hernández-Ruiz, J., García-Cánovas, F., Thorneley, R. N. F., Acosta, M., and Arnao, M. B. (1997) *J. Biol. Chem. 272*, 5469−5476.
44. Hernández-Ruiz, J., Arnao, M. B., Hiner, A. N. P., García-Cánovas, F., and Acosta, M. (2001) *Biochem. J. 354*, 107−114.
45. Hiner, A. N. P., Hernández-Ruiz, J., Rodríguez-López, J. N., Arnao, M. B., Varón, R., García-Cánovas, F., and Acosta, M. (2001) *J. Biol. Inorg. Chem. 6*, 504−516.
46. Hiner, A. N. P., Hernández-Ruiz, J., Rodríguez-López, J. N., García-Cánovas, F., Brisset, N. C., Smith, A. T., Arnao, M. B., and Acosta, M. (2002) *J. Biol. Chem. 277*, 26879−26885.
47. García-Meseguer, M. J., Vidal, J. A., García-Cánovas, F., Havsteen, B. H., García-Moreno, M., and Varón, R. (2001) *Biosystems 59*, 197−220.

BI034580Z